Electronic Supplementary Information

A Dynamic 3D DNA Nanostructure Based on Silicon-Supported Lipid Bilayers: The Highly Efficient DNA Nanomachine for Rapid and Sensitive Sensing

Zhi-Bin Wen, Xin Peng, Ze-Zhou Yang, Ying Zhuo, Ya-Qin Chai, Wen-Bin Liang*

and Ruo Yuan*

Key Laboratory of Luminescent and Real-Time Analytical Chemistry (Southwest University), Ministry of Education, College of Chemistry and Chemical Engineering, Southwest University, Chongqing 400715, PR China

* Corresponding author. Tel.: +86-23-68252277; Fax: +86-23-68253172

E-mail address: wenbinliangasu@gmail.com; yuanruo@swu.edu.cn

Table of Contents

Experimental Section

Chemicals and Materials. Magnesium acetate and glacial acetic acid were obtained from Sinopharm Chemical Reagents, Co., Ltd. (Shanghai, China). Tris was purchased from BBI Life Science Co. (Shanghai, China). 1 × TAMg buffer is composed of 45 mM Tris and 12.6 mM $Mg(OAc)_2 \cdot 6H_2O$. The silica beads (1 μm) and 1, 2-dioleoyl-sn-glycero-3-phosphocholine (DOPC) was purchased from Aladdin Industrial Co., Ltd. (Shanghai, China). 3-Aminopropyltriethoxysilane (APTES) was obtained from Sigma-Aldrich Co. (St. Louis, USA). Phosphate buffer saline (PBS), Dulbecco's modified eagle's medium (DMEM) and other cell culture products were purchased from Dingguo Biological Technology Co., Ltd. (Chongqing, China). The cervical cancer Hela cells and human breast cancer MCF-7 cells were purchased from the Type Culture Collection of the Chinese Academy of Sciences (Shanghai, China). All the other chemicals were of analytical grade and used without further purification. Ultrapure water with a resistivity of 18.2 MΩ/cm was used throughout this study.

All oligonucleotides were custom-synthesized by Dalian TaKaRa Holdings Inc. (Dalian, China). The sequences information was listed as Table S1. The binding sequences of microRNA-21, H_1, H_2, and H_3 are labeled with different color or model. Before use, the hairpin nucleotides (H_1, H_2, and H_3) were heated to 95 °C for 2 min and then cooled to room temperature to form stem-loop structure.

Table S1. Oligonucleotide sequences used in this work.

Names	Sequences (5'-3')
microRNA-21	UAG CUU AUC AGA CUG AUG UUG A

H_1	CGA GTG ACT GTC AAC ATC AGT CTG ATA AGC TAC AGT CAC TCG ATC CAA TCT ACA GCT TTT TTT TTT - Cholesterol
H_2	Cholesteryl - TTT TTT TTT TGC TGT AGA *TTG GAT CGA GTG ACT GCC ATG AGA TCA CGA TCC AAT CTA CAG C* - FAM
H_3	TAMRA - *GCT GTA GAT TGG ATC GTG ATC TCA TGG CAG TCA CTC GAT CCA A*CC ATG AGA TCA TTT TTT TTT T - Cholesterol
microRNA-141	UAA CAC UGU CUG GUA AAG AUG G
microRNA-155	UUA AUG CUA AUC GUG AUA GGG GU

Notes: The binding sequences between microRNA 21 and H1 were highlighted in red color; the binding sequences between H1 and H2 were highlighted with wave underline; the binding sequences between H2 and H3 were highlighted with Italic type model.

Apparatus. Fluorescence was recorded on a F-7000 fluorescence spectrophotometer (Hitachi, Tokyo, Japan). Gel Doc XR$^+$ System (Bio-Rad, U.S.A) was used to take images of polyacrylamide gels. The dynamic light scattering measurement was performed on a Malvern Zetasizer Nano ZS apparatus (Malvern, UK). The pH measurements were carried out with a pH-3C digital pH-meter (Shanghai LeiCi Device Works, China). The scanning electron microscope (SEM) characterization was performed on a scanning electron microscope (Hitachi, Japan). The transmission electron microscope (TEM) characterization was provided with a transmission electron microscope (FEI Co., U.S.A). Laser confocal microscopy measurements were performed by laser confocal microscope (Leica Microsystem Inc., Germany).

Preparation of DNA Nanomachine. A chloroform solution of DOPC (1 mg/mL) is dried overnight under vacuum, and the obtained lipid film is then hydrated using 1 × TAMg buffer through vortex mixing. Then the solution was extruded through a

polycarbonate (PC) membrane with a pore diameter of 1 μm for more than 35 times. The resulting bilayer solution was kept at 4 °C. Silico-supported bilayers are generated by mixing a solution of silica beads at a concentration of 9×10^6 particles/mL in PBS buffer, with an equal volume of bilayer solution in the same buffer for 30 minutes. The silica-supported bilayers solution is then washed by centrifugation (3× at 7000 rpm for 10 minutes) and the resulting pellet is re-suspended in 1× TAMg buffer. For the preparation of DNA nanomachine, H_1 (100 nM), H_2 (500 nM) and H_3 (500 nM) were incubated with the silica-supported bilayers solution for 15 minutes with gently stir at room temperature for the construction of DNA nanomachine. Then, the DNA nanomachine was washed by centrifugation (1× at 7000 rpm for 10 minutes) and the resulting solution is re-suspended in 1× TAMg buffer.

Preparation of Amino-functionalized Silica Nanoparticles. The silica colloidal (9×10^6 particles/mL) dispersion was functionalized with APTES by quickly added 0.3 ml of APTES with a vigorously stirring. The mixture was stirred overnight. The nanoparticle was purified by centrifugation and re-dispersion in ethanol. Above procedure was repeated three times.

Native polyacrylamide gel electrophoresis (PAGE). Firstly, 10 μL of each sample were mixed with 2 μL of 6 × loading buffer. And then, 10 μL of mixture was transferred into the gel electrophoresis system, respectively. Electrophoresis was performed in 1 × TBE (pH 8.0) at a 120 V constant voltage. The gels were then stained with ethidium

bromide for 20 min, followed by photographing with the Gel Doc XR^+ System.

Cell Culture. The cervical cancer Hela cells and human breast cancer MCF-7 cells were purchased from the Type Culture Collection of the Chinese Academy of Sciences (Shanghai, China). Hela and MCF-7 cells were grown in Dulbecco's modified Eagle medium (DMEM) containing 10% fetal bovine serum, 1% non-essential amino acids and 10 mg mL^{-1} insulin. All of the cells maintained in a humidified atmosphere of 5% CO_2 at 37 °C.

Confocal Fluorescent Imaging. MCF-7 cells and Hela cells were added into a 35 mm^2 Petri dish with 1 mL of culture medium at 37 °C for 24 h to reach 80% confluence. Then, the DNA nanomachines were delivery into cells and incubated for 3 h. After washing three times with 1 mL of PBS, the cells were incubated with 1 mL of fresh medium at 37 °C before imaging. The cellular images were acquired using a 20× objective. An Ar^+ laser (488 nm) was used as an excitation source for a FAM-labeled H_2 with a 520 nm (±10 nm) bandpass filter and a 580 nm (±10 nm) was used for fluorescent detection. The fluorescent images were presented by laser confocal microscopy.

Feasibility Investigation of the DNA Nanomachine. The polyacrylamide gel electrophoresis (PAGE) experiments were carried out to demonstrate the reaction ability of nucleic acids of DNA nanomachine with miRNA-21 as a target model. As shown in Figure S1A, lane 1, lane2 and lane 3 represented H_1, H_2, and H_3, respectively. The mixture of H_1, H_2 and H_3 was in lane 4, in which three distinct bands indicated that, in absence of miRNA-21, the proposed DNA nanomachine could coexist without any reactions. H_1 and target was in lane 5, in which the distinct band demonstrated the formation of the walker. Further incubation of H_1, H_2 and target led to formation of the scaffold (lane 6). Moreover, lane 7 represented the mixture of H_1, H_2, H_3 and target, two distinct bands indicated that the formation of the signal duplex and the walker. The results of PAGE suggested the DNA nanomachine could be triggered by miRNA-21, and the walker, scaffold and signal duplex were stable nanostructures.

Furthermore, the fluorescent response of the DNA nanomachine to target miRNA-21 was demonstrated by measurement of fluorescence of several samples with the excitation wavelength of 488 nm. As shown Figure S1B, H_1 showed no fluorescence as expected (curve a). FAM-labeled H_2 showed a strong fluorescent intensity at 520 nm (curve b) for the fluorescence emission of FAM. TAMRA-labeled H_3 showed fluorescence emission of TMARA at 580 nm (curve c). The mixture of H_1, H_2 and H_3 in the absence of the target miRNA-21 (curve d) exhibited a weak FRET signal, in which fluorescent intensity of FAM at 520 nm (I_{FAM}) was much larger than fluorescent intensity of TAMRA at 580 nm (I_{TMARA}). Further incubation of H_1, H_2, H_3 and 1 nM target miRNA-21 (curve e), a significantly amplified FRET signal could be observed,

the I_{TMARA} was increased along with the decreased I_{FAM} compared to curve d. These results demonstrated the signal response of DNA nanomachine to miRNA-21.

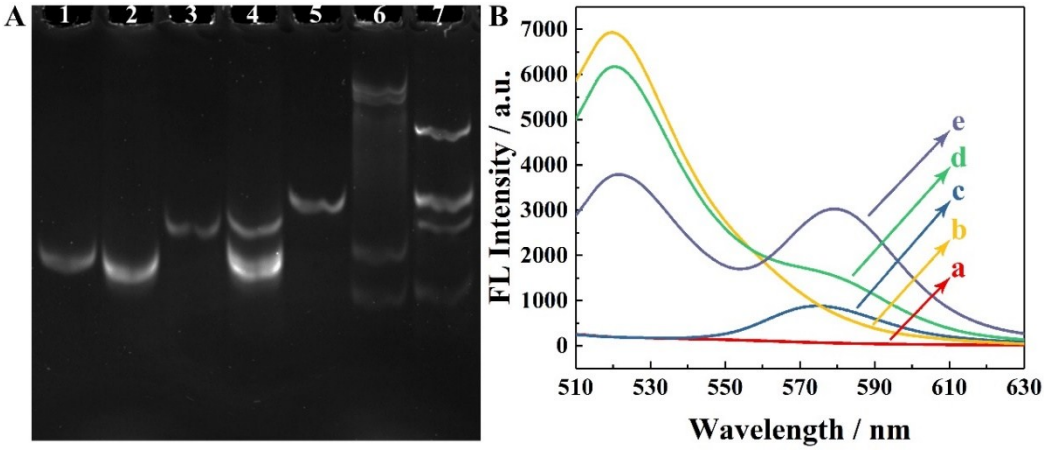

Figure S1. (A) Characterization of the proposed DNA nanomachine by PAGE. Lane 1: H_1, lane 2: H_2, lane 3: H_3, lane 4: $H_1 + H_2 + H_3$, lane 5: H_1 + miRNA-21, lane 6: $H_1 + H_2$ + Target, lane 7: $H_1 + H_2 + H_3$ + Target. (B) Typical fluorescence emission spectra of different samples: (a) H_1, (b) H_2, (c) H_3, (d) $H_1 + H_2 + H_3$, (e) $H_1 + H_2 + H_3$ + Target. All the solutions was excited at 488 nm.

Schematic illustration of Two Control Experiments. As illustrated in Scheme S1, two control experiments (Type I and Type II) were selected to verify the detection performance of the proposed DNA nanomachine. Type I is a traditional entropy-driven DNA nanomachine on silica beads *via* bonding carboxyl-modified H_2 onto amino-functionalized silica nanoparticle (Scheme S1A). Type II is a hairpin-catalytic detection system in PBS buffer (Scheme S1B).

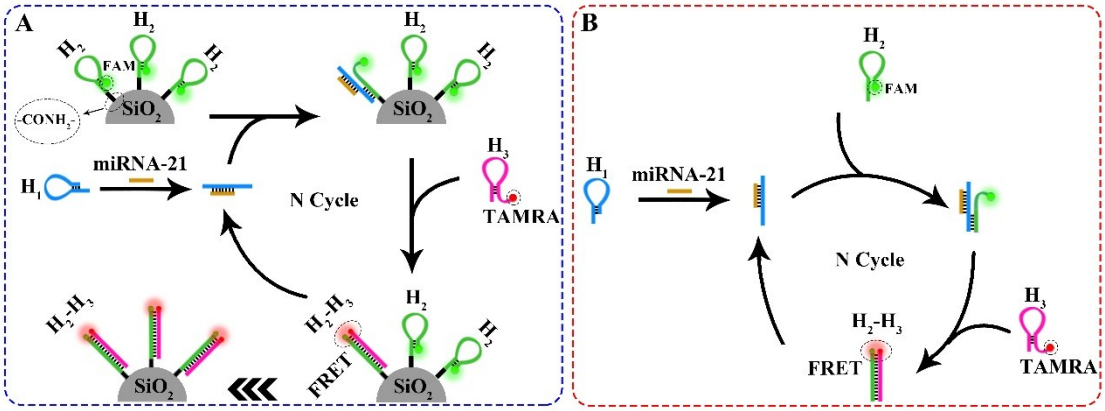

Scheme S1. Schematic illustrating the two control designs, Type I (A) and Type II (B).

Figure S2A, S2B and S2C were typical fluorescence emission spectra of the proposed DNA nanomachine, Type I and Type II reacted with 10 nM miRNA-21 in different incubation time from 0 to 60 min (curve a to g), respectively.

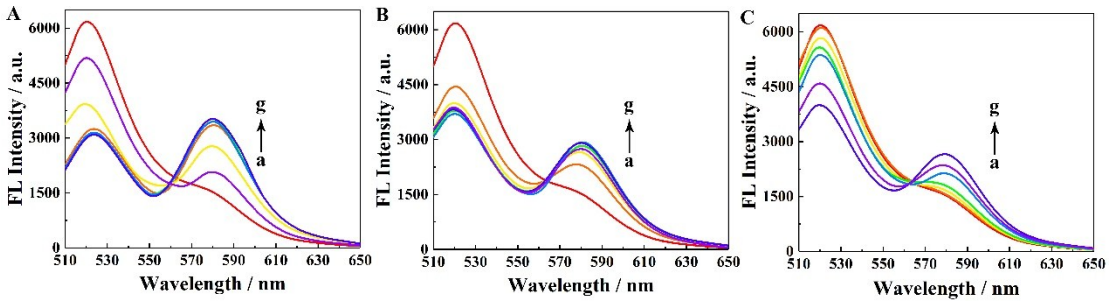

Figure S2. Typical fluorescence emission spectra of the proposed DNA nanomachine (A), Type I (B) and Type II (C) with 10 nM miRNA-21 as target at different incubation time. (a) 0 min, (b) 10 min, (c) 20 min, (d) 30 min, (e) 40 min, (f) 50 min, (g) 60min.

Equations Derivation of Kinetic Study. Based on the Briggs-Haldane model, we defined H2 + H3 as *S*, miRNA-21-H1 as *E*, H2-H3-miRNA-21-H1 as *ES* and H2-H3 as *P*. Therefore, the equation (4) could be demonstrated as equation (S1). Moreover, in the reaction, *E* existed as free state or hybrid state and would not be consumed, therefore, the sum of free state *E* (c_E) and hybrid state *E* (c_{ES}) is equal to initial *E* (c_{E_0}) and total *E* (c_{E_t}), which could be demonstrated as equation (S2).

$$S + E \underset{k_{-1}}{\overset{k_1}{\rightleftharpoons}} ES \overset{k_2}{\rightleftharpoons} P + E \tag{S1}$$

$$c_E + c_{ES} = c_{E_0} = c_{E_t} \tag{S2}$$

When the reaction is in steady state, the generation rate of *ES* (v_f) is equal to decomposition rate of *ES* (v_d), which could be demonstrated as equation (S3). Then equation (S4) could be obtained by rearranging the equation (S3). The result of $\frac{k_{-1} + k_2}{k_1}$ is a constant, and could be defined as k_m, which could be demonstrated as equation (S5). Then substituting equation (S5) into equation (S4), equation (S6) could be obtained.

$$\frac{d\, c_{ES}}{\mathrm{d\,t}} = v_f - v_d = k_1 \times (c_{Et} - c_{ES}) \times c_S - c_{ES} \times (k_{-1} + k_2) = 0 \tag{S3}$$

$$\frac{\left(c_{E_t} - c_{ES}\right) \times c_S}{c_{ES}} = \frac{k_{-1} + k_2}{k_1} \tag{S4}$$

$$\frac{k_{-1} + k_2}{k_1} = k_{\mathrm{m}}$$

(S5)

$$c_{ES} = \frac{c_{E_t} \times c_S}{k_{\mathrm{m}} + c_S}$$

(S6)

Furthermore, in this model, initial rate of reaction depended on c_{ES} and k_2, which could be demonstrated as equation (S7). Besides, as equation (S8) illustrated, when c_S was much more than c_E, the c_{ES} was equal to c_{E_t}, and v_0 would reach maximum (v_{max}). Eventually, the formula of k_{m} could be obtain by substituting equation (S8) into equation (S7), and be illustrated in equation (S9). In this model, k_2 was much bigger than k_{-1} due to the accurate complementary base, which could be demonstrated as $k_2 \gg k_{-1}$. Hence, k_{m} could be illustrated as $k_{\mathrm{m}} = \frac{k_2}{k_1}$.

$$v_0 = k_2 \times c_{ES} = \frac{k_2 \times c_{E_t} \times c_S}{k_{\mathrm{m}} + c_S}$$

(S7)

$$\lim_{c_s \to \infty} v_0 = \frac{k_2 \times c_{E_t} \times c_S}{k_{\mathrm{m}} + c_S} = k_2 \times c_{E_t} = v_{max}$$

(S8)

$$k_{\mathrm{m}} = \left(\frac{v_{max}}{v_0} - 1 \right) \times c_S$$

(S9)

Selectivity of the Proposed DNA Nanomachine. To evaluate the selectivity of the proposed nanomachine, controlled trials were conducted by performing the detection method on different miRNA sequences (miRNA-141, miRNA-155, let-7a). As shown in Figure S3, the ratio intensity of mixed sample of miRNA-141, miRNA-155, let-7a and miRNA-21 is almost same as the ratio intensity of miRNA-21 sample. A significant signal decrease was observed when the sample was only miRNA-141, miRNA-155 or let-7a, and the ratio intensity was close to the blank sample, even though the concentration of potential interfering substances was 100 times higher than miRNA-21. These results indicated that the proposed DNA nanomachine possesses excellent selectivity toward miRNA-21 rather than other interference sequences.

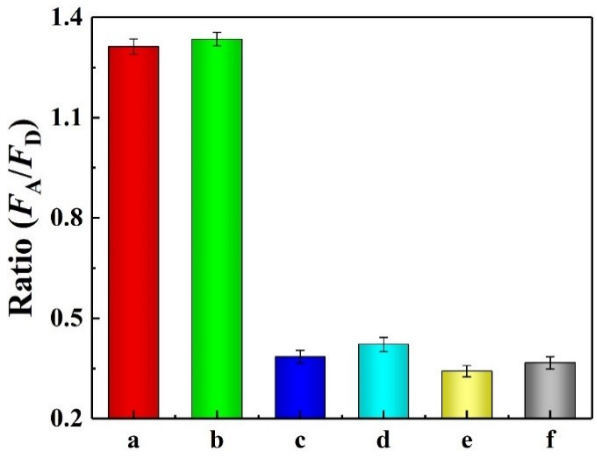

Figure S3. Specificity of the proposed nanomachine for miRNA-21: (a) miRNA-21 (10 nM), (b) mixed sample, (c) miRNA-141 (1 μM), (d) miRNA-155 (1 μM), (e) let-7a (1 μM), (f) blank sample. F_A and F_D was fluorescence intensity of acceptor and donor.

Biocompatibility of the Proposed DNA Nanomachine. In this work, the biocompatibility of the proposed nanomachine was evaluated based on the MTT assay with MCF-7 cells. Typically, the cells were cultured to 5 × 10^3 cells/well, and the proposed nanomachine with various dilutions was added in the wells for an additional 24 h incubation. And then, 20 μL MTT solution (5 mg/mL in PBS) was added to each wells for further 4 h incubation to transfer MTT to formazan crystals by living cells. Finally, after removing the medium with MTT carefully, 150 μL dimethylsulfoxide (DMSO) was added to each well to dissolve the formazan crystals, which was evaluated by Multiskan Spectrum microplate reader at 570 nm. And thus, the survival fraction could be calculated via the equation: survival fraction $= \frac{I_{\text{test}} - I_{\text{black}}}{I_{\text{control}} - I_{\text{black}}} \times 100\%$ (I_{test} was the mean intensity of the test wells, I_{black} was the mean intensity of the black wells and I_{control} was the mean intensity of the control wells). As shown in Figure S4, the survival fraction was above 85%, even the proposed nanomachine without dilution was employed, indicating the suitable biocompatibility of the proposed nanomachine.

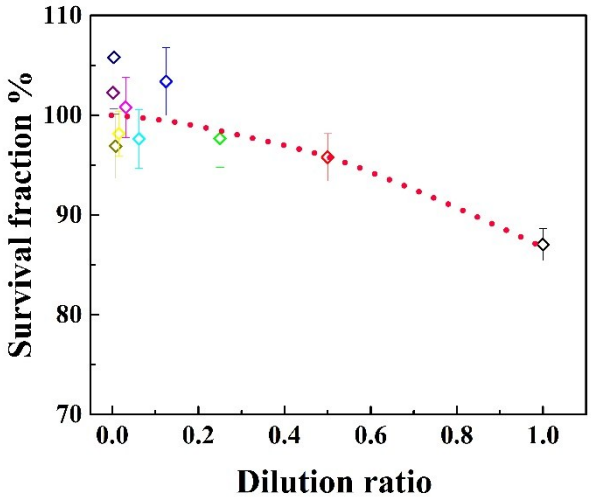

Figure S4. Characterizations for the biocompatibility of the proposed nanomachine based on MTT

assay.

Table S2. Comparison of the proposed nanomachine for miRNAs detection with other detection methods.

Target	Detection method	Limit of Detection	Linear range	Ref.
TK1	Fluorescence	18 pM	0.05 nM-100 nM	1
miRNA-141	Fluorescence	25 pM	200 pM-150 nM	2
miRNA-122	Fluorescence	5 nM	5 nM-1000 nM	3
miRNA-21	Fluorescence	10 pM	50 pM-300 nM	4
miRNA-21	Fluorescence	47 pM	0.15 nM-16 nM	5
miRNA-21	Fluorescence	0.68 pM	2 pM-10 nM	This work

References:

1. J. Huang, H. Wang, X. Yang, K. Quan, Y. Yang, L. Ying, N. Xie, M. Ou and K. Wang, *Chem*. *Sci*., 2016, **7**, 3829-3835.
2. Y. Yang, J. Huang, X. Yang, X. He, K. Quan, N. Xie, M. Ou and K. Wang, *Anal*. *Chem*., 2017, **89**, 5850-5856.
3. R. Liao, K. He, C. Chen, X. Chen and C. Cai, *Anal*. *Chem*., 2016, **88**, 4254-4258.
4. Y. Wu, J. Huang, X. Yang, Y. Yang, K. Quan, N. Xie, J. Li, C. Ma and K. Wang, *Anal*. *Chem*., 2017, **89**, 8377-8383.
5. S. J. Zhen, X. Xiao, C. H. Li and C. Z. Huang, *Anal*. *Chem*., 2017, **89**, 8766-8771.